CYCLIC TESTS ON BOLTED AND WELDED BEAM-TO-COLUMN CONNECTIONS

Luis Calado* and Elena Mele**

* Associate Professor, Civil Engineering and Architecture Department (DECivil)
Instituto Superior Tecnico, Av. Rovisco Pais, 1049-001 Lisbon, Portugal
** Assistant Professor, Structural Analysis and Design Department (DAPS)
University of Naples "Federico II", P. le Tecchio 80, 80125 Naples, Italy

ABSTRACT

In this paper, the aspects characterising the Europe design practice in beam-to-column connections are reported, the differences between several typologies are underlined, and the main issues addressed in experimental programs performed during the 90's at Instituto Superior Técnico of Lisbon (Portugal) in collaboration with the Universitá di Napoli "Federico II" (Italy) are reviewed. The experimental programs were devoted to the assessment of the cyclic behaviour of small and full scale, European type, beam-column subassemblages with welded and bolted connections. Two alternative connection solutions, bolted and welded, designed for the same beam-to-column joints, are comparatively analysed. The bolted connections are top and seat with double web angles (TSW) connections, while the welded connections are both fully welded (WW) and welded flange with web cleats (WF) connections. The experimental results have evidenced the effect of the scale of the specimen, the influence of panel zone and of the loading history on the cyclic behaviour and failure modes of the connections. The major outcomes of these experimental investigations are also evaluated through the comparison with the test results obtained in other research programs.

KEYWORDS: Connections, Cyclic Behaviour, Experimental Tests, Bolted, Welded

INTRODUCTION

During the 90's, several research programs have been developed world-wide in the field of seismic behaviour of steel structures in order to enrich the experimental database and for assessing the major parameters affecting the cyclic behaviour of beam-to-column connections.

Bolted connections, in particular top and seat with web angles (TSW) connections, have not traditionally been considered appropriate in seismic applications, due to the partial strength and semi-rigidity characteristics. Therefore, TSW connections, though extensively investigated in the monotonic range, as reported in Kishi and Chen (1990), received less attention in the cyclic range.

Only recently, it has been pointed out (Astaneh, 1995; Elnashai et al., 1998) that the dynamic behaviour semi-rigid frames can be particularly favourable due to the period elongation, related to the connection flexibility, and to the damping increase, related to highly dissipative friction mechanism deriving from a proper "slip capacity design". Both these effects act as a sort of self-isolation of the frame structure, thus leading to remarkable reduction of the seismic actions. It is worth to emphasise that also in the context of the SAC steel project, started immediately after the Northridge earthquake to address the specific problems of beam-to-column connections, a great interest in bolted configurations as alternative to the standard welded connections (Roeder, 1998), can be found.

In this research framework, a wide experimental activity on different types (welded and bolted) of beam-to-column connections has been carried out at the Material and Structures Test Laboratory of the Instituto Superior Técnico (IST) of Lisbon in last few years. The experimental tests have been performed on specimens representative of frame structure beam-to-column joints close to the ones typical of European design practice. Some results have been already presented (Mele et al., 1997; Calado et al., 1999a, 1999b; Calado and Mele, 2000).

In this paper, an overview on the major experimental researches developed at the IST during the second half of the 90's is presented.

OBJECT AND AIMS OF THE PAPER

In this paper, some results obtained in the framework of the recent experimental activity carried out at the IST on beam-to-column connections are provided. In particular, two alternative connection solutions, bolted and welded, designed for the same beam-to-column joints, are comparatively analysed. The bolted connections are top and seat with double web angles (TSW) connections, while the welded connections are both fully welded (WW) and welded flange with web cleats (WF) connections.

The connection specimens tested at IST are in the following appointed as "small size" or "large size" specimens, depending on the size of the cross sections of the connected beam and column, since some aspects of the observed behaviour can be related to the specimen size.

In particular, the effect of the member cross section size is mainly assessed with reference to the monotonic behaviour, while the results obtained from both monotonic and cyclic tests are utilised for describing and examining the major phenomena which govern the behaviour of bolted and welded connections and for comparatively assessing the effect of the design and of the loading history on the connection performance. Some conclusions based on these results are also confirmed by the comparison to analogous test results available in the inherent bibliography.

Table 1: Typology and Scale of the Specimens

NAME	BCC1	BCC4	BCC5	BCC6	BCC8	BCC7	BCC9	BCC10
Typology	TSW	WF	WW	WW	WW	TSW	TSW	TSW
Scale	Small	Small	Large	Large	Large	Large	Large	Large
Beam	HE120 A	HE120 A	IPE300	IPE300	IPE300	IPE300	IPE300	IPE300
Column	HE120 A	HE120 A	HE160 B	HE200 B	HE240 B	HE160 B	HE200 B	HE240 B

THE TESTED SPECIMENS

In Table 1, the examined specimens are identified according to the connection typology and to the scale; further, the beam and column cross sections of the specimens are reported. In the following a brief description of the geometry of the specimens, of the connection details and of the material properties is provided.

1. Small Scale Specimens

The BCC1 and BCC4 are small scale, respectively TSW and WF, specimens. Each specimen is a single-sided beam-to-column joint, made of a 1238 mm long beam attached to a 1476 mm long column. As already reported in Table 1, both column and beam sections used in the specimens are HE120A (depth = 114 mm). Arrangements and dimensions of the specimens are given in Figure 1. Continuity plates, fillet welded to the column web and flanges have been added in the column for reducing local deformations
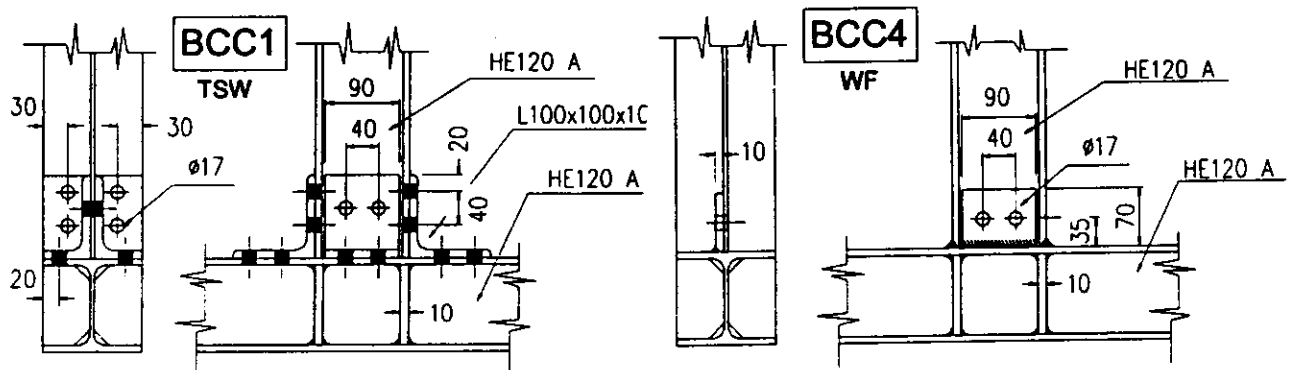

Fig. 1 Small-scale specimens

The material used for the columns, beams, and angles is steel S235 JR, with nominal values of yield and ultimate stress respectively equal to $f_y = 235$ MPa and f_u MPa. The bolts utilised in both connections are $M16$ grade 8.8 (yield stress $f_{yb} = 640$ MPa, ultimate stress $f_{ub} = 800$ MPa, $A_s = 157$ mm^2), preloaded according to the EC3 (CEN 1997) provisions, i.e. at $F_{P,CD} = 0.7 f_{ub} A_s = 87.9$ kN.

Table 2: Threshold Moment Capacities (in kNm) of the Small-Scale TSW Specimen BCC1 (Nominal and Actual Values)

	M_{slip}	$M_{y,angle}$	M_{pb}	M_{pc}
Nominal values	12.0 - 18.0	15.3	28	28
Actual values		21.5	40	40

2. TSW Specimens

In the BCC1 (TSW) specimen, 100x100x10 angles have been adopted. Two rows of bolts are placed on each leg of the flange angles, while on the legs of the web angles, there is only one row of two bolts. It is well known that two major phenomena characterise the behaviour of the TSW connection: the slippage of bolts and the yielding of the tension angle. The BCC1 specimen has been designed as a not "slip critical" connection, since slippage of top and seat angle bolts occurs at a load level lower than the one corresponding to yielding of the tension angle. In Table 2, the bending moment corresponding to the two above behaviour thresholds (slip $\left(M_{slip}\right)$ and angle yielding $\left(M_{y,angle}\right)$ are reported together with the beam $\left(M_{pb}\right)$ and column $\left(M_{pc}\right)$ moment capacities. The values provided in the table have been computed with reference both to the nominal and to the actual values of the material strength derived from tension coupon tests.

3. WF Specimens

In the BCC4 (WF) specimen, the beam flanges have been connected to the column flange by means of complete joint penetration (CJP) groove welds, and web cleats have been welded to the column flange and connected by means of two bolts to the beam web. In the CPJ welded connections (WF and WW types), both the elastic response, i.e. the initial stiffness, and the inelastic behaviour, i.e. the strength and deformation capacity and the collapse mode, are strongly dependent on the strength ratios between the three components which frame in the joint, i.e. the beam, the column and the panel zone. In Table 3, the flexural strengths of the beam $\left(M_{pb}\right)$, column $\left(M_{pc}\right)$ and panel zone $\left(M_{p,PZ}\right)$, all computed on the basis both of the nominal yield stress $\left(f_y = 235 \text{MPa}\right)$ and of the actual yield stress obtained from coupon tests, are reported. The panel zone flexural strengths have been evaluated according to the Eurocode 3 (EC3) Annex J provisions (CEN, 1997). From the simple comparison among the plastic moment values reported in the table, it can be observed that in the BCC4 specimen, the weakest component of the joint configuration is the panel zone.

**Table 3: Moment Capacities (in kNm) of the Small-Scale WF Specimen BCC4 (Nominal and Actual Values)**

	M_{pb}	M_{pc}	$M_{p,PZ}$
Nominal values	28	28	15.8
Actual values	40	40	22.5

4. Large Scale Specimens

Two series of large-scale specimens have been designed and tested, namely a WW specimen series (BCC5, BCC6 and BCC8) and a TSW specimen series (BCC9, BCC7 and BCC10). The specimens of the two series are T-shaped beam-column subassemblages, consisting of a 1000 mm long beam and an 1800 mm long column. As in the small-scale specimens, the steel is S235 JR and the bolts utilised in the TSW connections are $M16$ grade 8.8, preloaded according to the EC3.
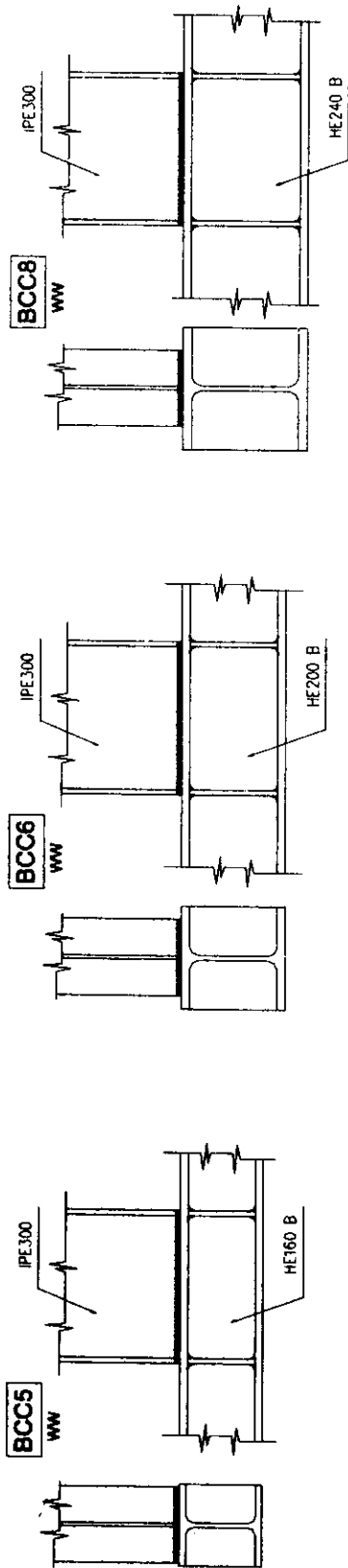
Fig. 2 Fully welded specimens
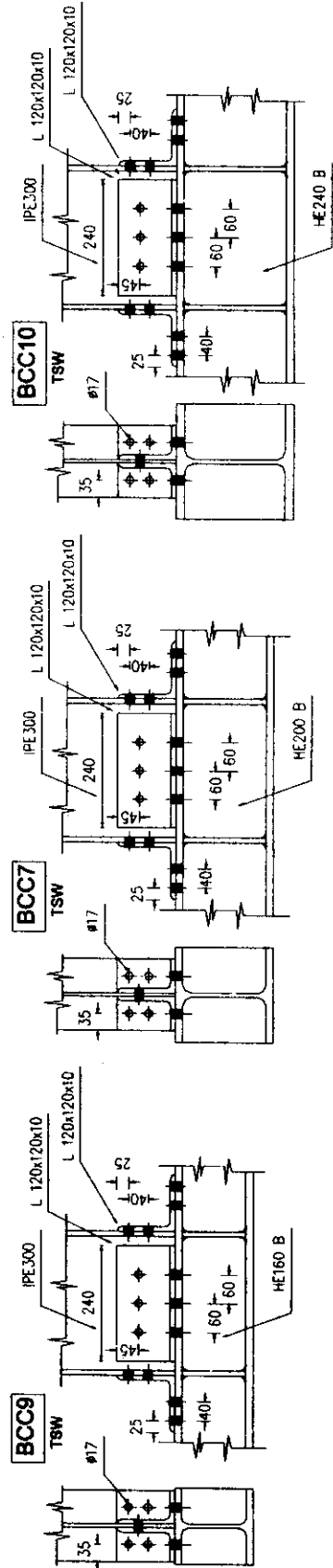
Fig. 3 Top and seat with double web angles specimens

As it can be derived from Table 1, in each series the cross section of the beam is the same (IPE300), while the column cross section has been varied, being respectively HE160B for the BCC5 (WW) and BCC9 (TSW) specimens, HE200B for the BCC6 (WW) and BCC7 (TSW) specimens, and HE240B for the BCC8 (WW) and BCC10 (TSW) specimens. In both the series, 10 mm thick plate stiffeners have ensured the continuity of the connection through the column, fillet welded to the column web and flanges. Arrangements and dimensions of the WW and TSW specimens are respectively given in Figures 2 and 3.

Table 4: Moment Capacities (in kNm) of the Large-Scale WW Specimens
(Nominal and Actual Values)

		M_{pb}	M_{pc}	$M_{p,PZ}$
BCC5	Nominal values	147.6	83.2	91.1
	Actual values	172.6	114.4	149.8
BCC6	Nominal values	147.6	151.1	132.4
	Actual values	175.0	201.0	220.7
BCC8	Nominal values	147.6	247.5	182.9
	Actual values	183.0	316.0	239.7

5. WW Specimens

In the WW specimens, the beam flanges have been connected to the column flange by means of complete joint penetration (CJP) groove welds, while fillet welds have been applied between both sides of the beam web and the column flange. The beam flange welds are double bevel complete joint penetration (CJP) butt welds, with no backing bars. Manual Metal Arc (MMA) welding process has been used with electrodes AWS 5.1 E 7018-1. Welding for the beam top and bottom flanges are both performed in the flat position; thus, the root of the CJP welds is located on the interior side of both the top and the bottom flange.

As in the case of the small scale welded specimen, also for the large scale BCC5, BCC6 and BCC8 specimens, the flexural strengths of the beam (M_{pb}), column (M_{pc}) and panel zone $(M_{p,PZ})$, have been computed on the basis of the nominal and actual yield stress and are reported in Table 4. From the simple comparison among the nominal plastic moments reported in Table 4, it can be observed that in the three WW specimens, the weakest component of the joint configuration is respectively: the column for the BCC5 specimen, the panel zone for the BCC6 specimen, and he beam for the BCC8 specimen.

Table 5: Threshold Moment Capacities (in kNm) of the Large-Scale TSW Specimen
(Nominal and Actual Values)

		M_{slip}	$M_{y,angle}$	M_{pb}	M_{pc}
BCC9	Nominal values	32-47.5	23.3	147.6	83.2
	Actual values		28.1	198.2	123.4
BCC7	Nominal values	32-47.5	23.3	147.6	151.1
	Actual values		28.1	198.2	194.4
BCC10	Nominal values	32-47.5	23.3	147.6	247.5
	Actual values		28.1	198.2	305.7

6. TSW Specimens

In the BCC9, BCC7 and BCC10 (TSW) specimens, 120x120x10 angles have been adopted. Two rows of bolts are placed on each leg of the flange angles, while on the legs of the web angles, there is only one row of three bolts. As in the case of small scale TSW specimens, the bending moment corresponding to bolt slippage (M_{slip}) and angle yielding $(M_{y,angle})$ have been computed with reference to the nominal values of the material strength and are reported in Table 5, together with the beam (M_{pb}) and column

(M_{pc}) moment capacities. The TSW large-scale specimens are "slip critical" connections, since slippage of top and seat angle bolts occurs at a load level higher than the one corresponding to yielding of the tension angle.

Table 6: Average Test Values of Material Properties

| Specimen type	Component	f_y [MPa]	f_u [MPa]	YR
BCC1 BCC4	Beam/Column web (HE120A)	334	451.5	1.35
	Beam/Column flanges (HE120A)	336.5	447	1.33
BCC1	Angles	331	468	1.41
BCC5	Beam flange	274.8	404.6	1.47
	Beam web	305.5	412.6	1.35
	Column flange	323.1	460.2	1.42
	Column web	395.6	490.1	1.24
BCC6	Beam flange	278.6	398.8	1.43
	Beam web	304.9	411.4	1.35
	Column flange	312.6	434.9	1.39
	Column web	401.6	489.8	1.22
BCC8	Beam flange	292	445	1.53
	Beam web	300	450	1.50
	Column flange	300	457	1.52
	Column web	309	469	1.52
BCC9 BBC7 BCC10	Beam flange	304.7	452.6	1.48
	Beam web	315.7	451.3	1.49
	Angle	284	420.1	1.48
BCC9	Column flange	303.4	453.1	1.49
	Column web	348.6	490.3	1.41
BCC7	Column flange	282.3	433.3	1.53
	Column web	302.3	434.4	1.44
BCC10	Column flange	304.7	454.4	1.49
	Column web	290.3	447.9	1.54

MATERIAL TENSION TESTS

The basic monotonic stress-strain properties of the specimen materials have been determined through coupon tension tests. In Table 6, the average stress values, which have been used for computing the actual values of the strength properties of the specimens, are provided. In particular, the yield stress value (f_y), the maximum value of the stress recorded in the test (f_u), and the yield ratio (YR) are given for the beam (flanges and web), for the column (flanges and web), and, in the case of TSW specimens, for the angles.

EXPERIMENTAL SET-UP, INSTRUMENTATION AND LOADING HISTORIES

The test set-up, represented in Figure 4, mainly consists in a foundation, a supporting girder, a reaction RC wall, a power jackscrew and a lateral frame. The power jackscrew (capacity 1000 kN, stroke 400 mm) is attached to a specific frame, pre-stressed against the reaction wall and designed to accommodate the screw backward movement. The specimen is connected to the supporting girder through two steel elements. The supporting girder is fastened to the reaction wall and to the foundation by means of pre-stressed bars.
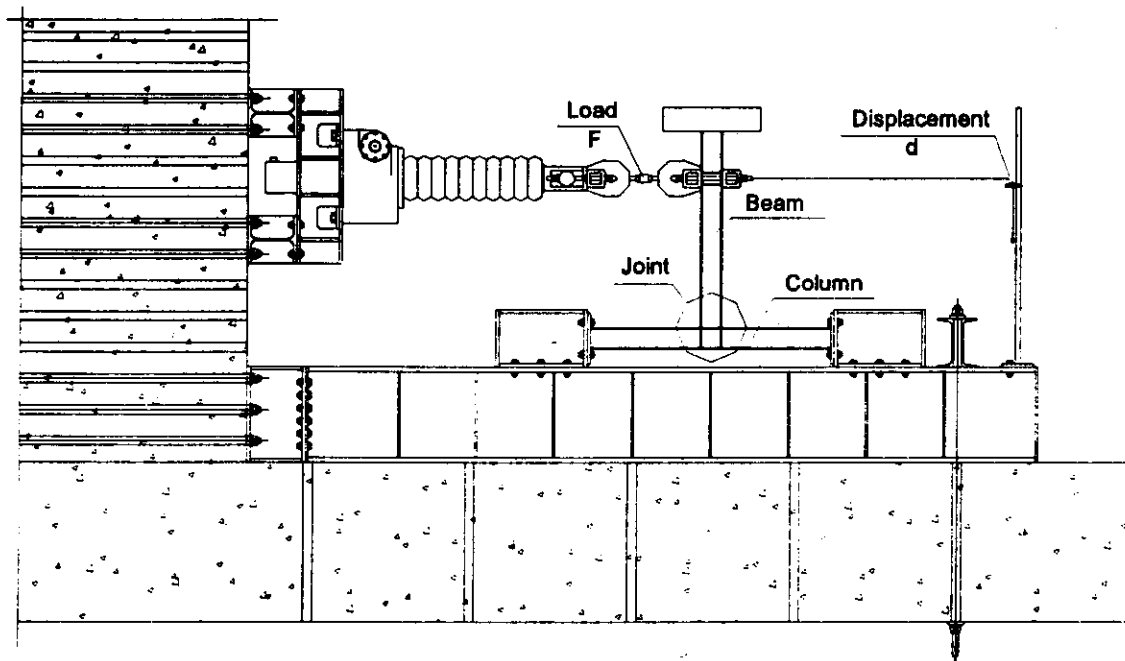
Fig. 4 Experimental set-up

An automatic testing technique was developed to allow computerised control of the power jackscrew, of the displacement and of all the transducers used to monitor the specimens during the testing process. Specimens have been instrumented with electrical displacement transducers (LVDTs), which record the displacement histories at several points in order to obtain a careful documentation of the various phenomena occurring during the tests. The same arrangement of LVDTs has been adopted for the different specimen types. The typical instrumentation set-up is the one provided in Figure 5.
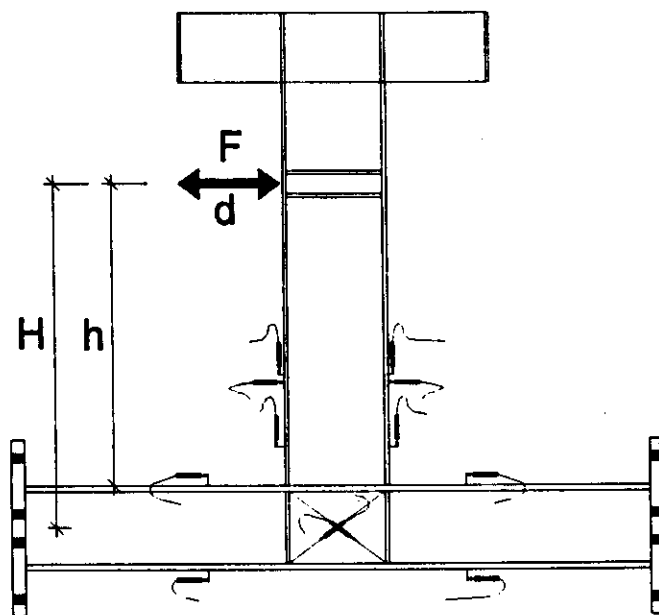

Fig. 5 Instrumentation of the specimens

Different rotation histories have been used in testing the specimens. The complete sets of tests carried out on the small scale TSW and WF specimens, large scale WW specimens and large scale TSW specimens are given in Table 7, where the loading histories are defined in terms of total interstory drift

angle (d/H), i.e. applied beam tip displacement d normalised to the distance between beam tip and the centerline of the column H.

Table 7: Applied Displacement Histories d/H [%]

	BCC1	BCC4	BCC5	BCC6	BCC8	BCC9	BCC7	BCC10
A	± 10	+ 5 / - 15	± 5	± 5	± 5	± 5	± 5	± 5
B	± 15	Unsymm. ECCS	± 7.5	± 7.5	± 3.75	± 7.5	± 7.5	± 3.75
BB	-	-	± 7.5	± 7.5	-	-	-	-
C	± 7.5	± 7.5	ECCS	ECCS	± 7.5	± 3.75	ECCS	ECCS
D	± 15	± 5	± 3.75	± 3.75	ECCS	ECCS	± 3.75	± 7.5
E	+ 15 / - 5	± 6.25	Monotonic	Monotonic	± 3.75	Monotonic	Monotonic	Monotonic
F	Random	ECCS	-	-	Monotonic	-	-	-
G	ECCS	Monotonic	-	-	-	-	-	-
H	± 12.5	-	-	-	-	-	-	-
I	ECCS	-	-	-	-	-	-	-
J	Monotonic	-	-	-	-	-	-	-

MONOTONIC BEHAVIOUR OF THE SPECIMENS

1. Small Scale Specimens

The moment rotation curves obtained from the monotonic tests carried out on the two types of small scale connections are presented in Figures 6(a) and (b) in dimensional and non-dimensional form. In these curves, the moment is evaluated at column centreline and the rotation is given by the total interstory drift angle (d/H), i.e. the applied beam tip displacement (d) normalised to the distance between beam tip and the column centreline (H).

In Figure 6(a), the complete $M - d/H$ curves obtained from the tests are depicted together with two horizontal lines, which give the plastic $(M_{pb} = f_y W_{pl})$ and ultimate $(M_{ub} = f_{max} W_{pl})$ moment capacity of the beam, respectively computed by adopting the yield stress (f_y) and the maximum stress (f_{max}) resulting from beam flange coupon tests. In Figure 6(b), the initial part of the experimental curves is reported in non-dimensional form $m - \phi$, where, according to the definition provided in the EC3 for the classification of joints, the girder plastic moment, M_{pb}, and the non-dimensional girder stiffness $((EI_b/H)/M_{pb})$, have been respectively used for normalising moment and rotation values.

From the curves reported in Figure 6(a), it is evident that the connections are capable of providing large deformation capacities and that the bending strength of both the connections reaches the girder plastic moment. It has to be remarked, though, that the strength capacity of the two connection types is attained at different deformation levels.

The significant value of the bending strength (equal to the beam plastic moment) developed by the TSW (BCC1) connection, which is the type in principle closer to the ideally hinged behaviour, is related to the geometry of the connection components. In fact, quite large dimensions of the angles with respect to the beam depth as well as the two bolt rows on the legs of the angles give rise to a large lever arm. This geometry and arrangement of the connecting elements (angles and bolts) give rise to a large degree of restraint for the connected parts (i.e. beam and column), resulting in a particularly relevant strengthening effect. Therefore, the geometrical arrangements of this bolted specimen give rise to a full-strength joint, even though the slip phenomenon, which arises at load level lower than the maximum load sustainable by the specimen, leads to a semi-rigid behaviour.

In contrast, the monotonic curve for welded flange with bolted web connection, which should be the type closer to the ideally rigid behaviour, evidences some initial flexibility due to the effect of the panel zone deformability, thus the plastic moment of the beam is reached at very large values of rotation (20%). In this test, the specimen instrumentation was out of service at approximately 20% of global rotation, thus recording was interrupted at that deformation level. However in the test, the specimen reached higher rotations without collapse occurrence.
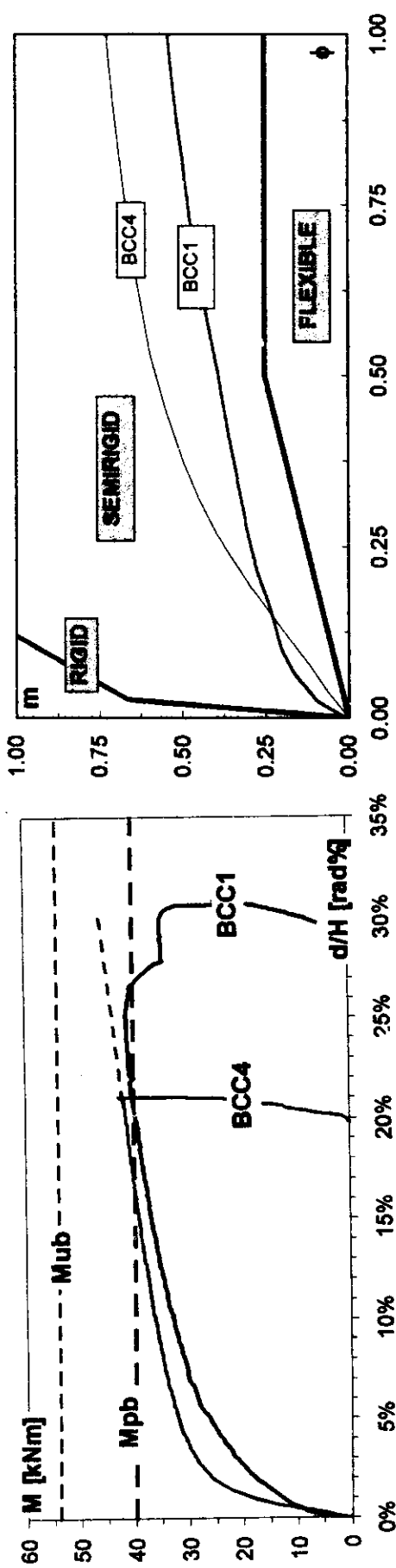
Fig. 6 Monotonic curves of small-scale specimens: (a) dimensional form (b) non-dimensional form
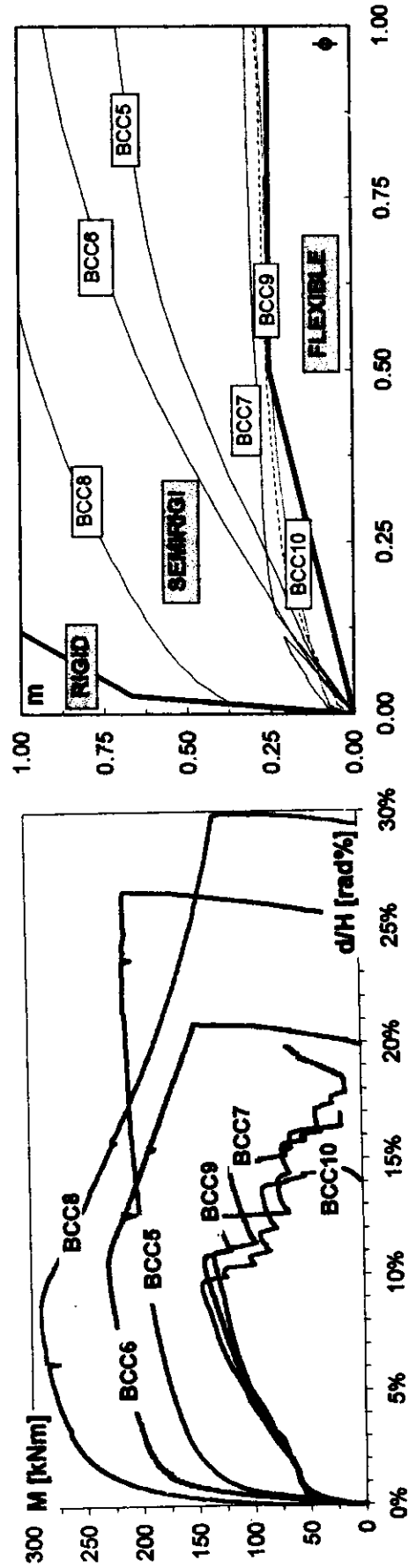
Fig. 7 Monotonic curves of large-scale specimens: (a) dimensional form (b) non-dimensional form
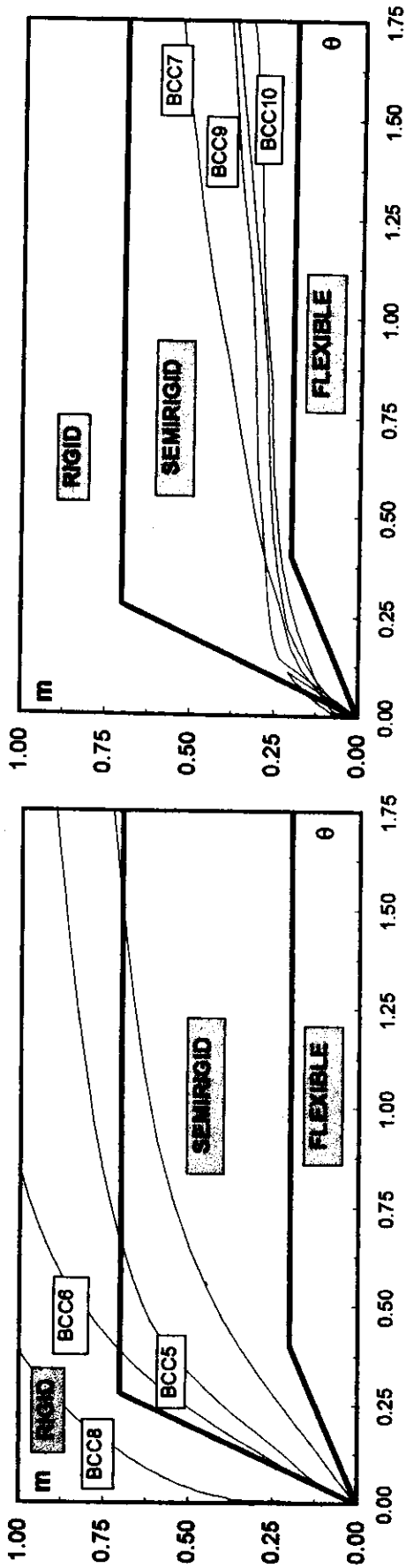
Fig. 8 Classification of (a) WW specimens and (b) TSW specimens according to Bjorhovde et al. (1990)
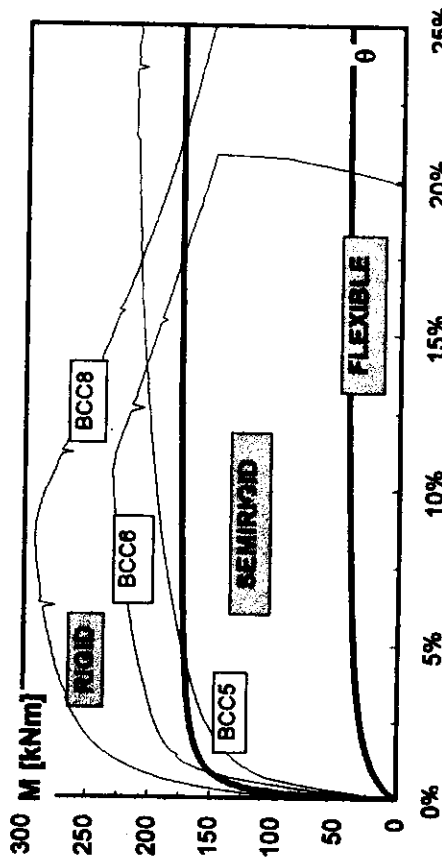
Fig. 9 Classification of (a) WW specimens and (b) TSW specimens according to Hasan et al. (1998)

In Figure 6(b), the initial part of the normalised experimental curves are reported in order to classify the connections on the basis of their initial stiffness according to the EC3. The two connections appear to be both of the semi-rigid type, even though different values of the non-dimensional strength are attained at $\phi = 0.5$, which can be considered a normalised threshold deformation level (approximately corresponding to $d/H = 1.5\%$). This last point demonstrates the importance of classifying the connection according both to stiffness and strength at specific performance (deformation) levels. Starting from this and other drawbacks related to the EC3 classification system, different classification systems of joints have been recently proposed by several researchers (Bjorhovde et al., 1990; Nethercot et al., 1998; Hasan et al., 1998). In the following, these proposals are discussed and some applications are provided.

2. Large Scale Specimens

Similarly to the small-scale specimens, in Figures 7(a) and 7(b), the moment rotation curves obtained from the monotonic tests carried out on the two series of large scale connections are provided in dimensional and non-dimensional form. From the experimental results on the two series of specimen, the effect both of the connection typology (TSW and WW) and of the column cross section (HE160B, HE200B, HE240B) can be envisaged.

By comparing the two series of experimental curves in the dimensional form, it must be noticed that the three WW specimens show significant differences in the initial stiffness, maximum strength and deformation capacity, thus demonstrating a strong effect of the column cross section size. On the contrary, the three TSW specimens present quite close experimental responses. This difference between the behaviour of WW and TSW specimens is mainly related to the design of the specimens, since in the TSW connections, the weakest component is the same in the three specimens (the angle in tension); thus, the beam, column and panel zone strength ratios do not affect the response of the specimens. Slight scatters can be observed in the initial stiffness, due to the different column and panel zone deformability, but the non-linear portion of the curve and the maximum bending moment are very similar.

As already evidenced, the behaviour of the WW connections is affected by the column dimensions since the three combinations of beam and column framing in the joint give rise to panel zone strength values respectively: smaller than, approximately equal to and larger than the plastic moment of the beam, for the BCC5, BCC6 and BCC8 specimens.

The above observation is confirmed by analysing the main experimental data provided in Table 8.

Table 8: Main Experimental Data from the Tests on the Large-Scale Specimens

		M [kNm]	M_b [kNm]	d/H [%]	Φ_{PZ} [%]	$\Phi_{b,pl} - \Phi_{PZ}$ [%]
WW	BCC5	214	196	21.4	16.5	0.66
	BCC6	231	207	10.5	4.5	4.9
	BCC8	292	251	8.3	3.3	5.3
		M [kNm]	M_b [kNm]	d/H [%]	Φ_{PZ} [%]	Φ_{slip} [%]
TSW	BCC9	135	122.5	10.8	2.4	5.2
	BCC7	144	127	10.5	1.15	6.8
	BCC10	146	126	9.4	0.19	4.8

In particular it can be noticed that while in the WW specimens, the panel zone distortion Φ_{PZ} significantly contributes to the specimen global rotation d/H (at the maximum value of the bending moment registered in the monotonic test), though at different extent in the three specimens, a completely different order of magnitude of this contribution is registered in the TSW connections. For the TSW specimens, instead, the rotations due to bolt slippage Φ_{slip} computed on the basis of the LVDTs measured displacements constitutes a major contribution to the total rotation d/H.

The Figure 7(b) shows that both the TSW and the WW specimens can be classified, according to the EC3, as semirigid joints, even though the TSW specimens are very close to the boundary of the flexible joint behaviour, while all the WW connections are able to sustain bending moment larger than the beam plastic moment capacity. Thus, even though WW specimens can be classified as full strength connections, they experience the maximum bending moment at large deformation levels.
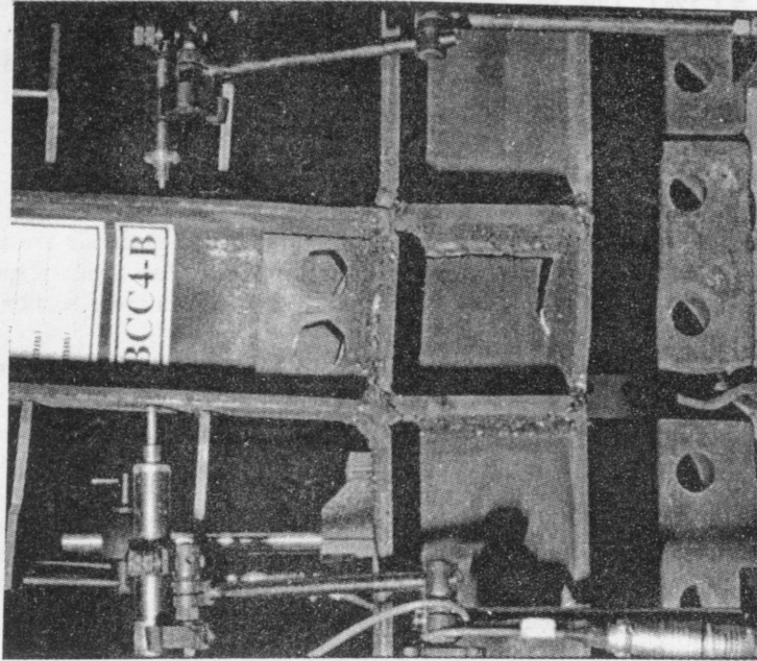
Fig. 11 Failure mode of the panel zone of a welded flange and web cleats connection (BCC4)
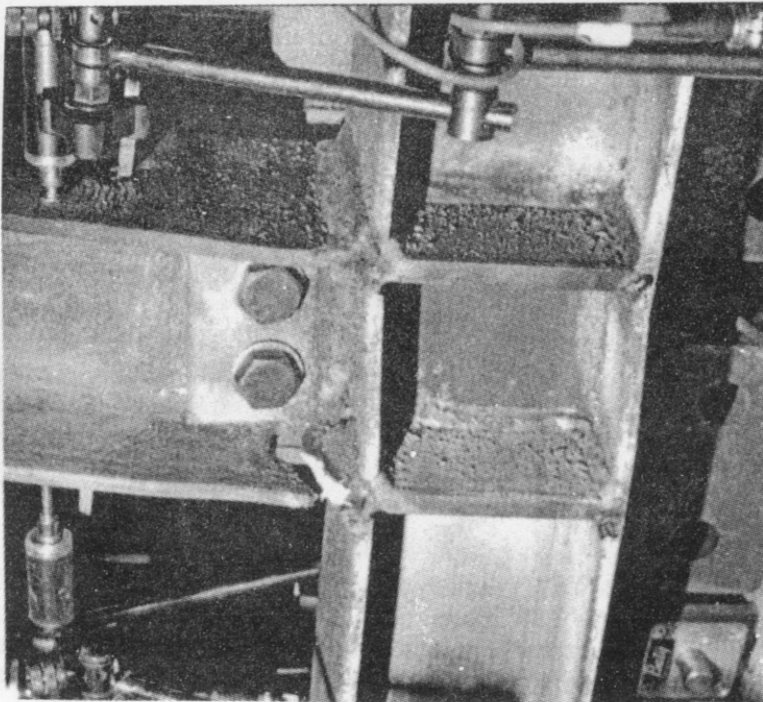
Fig. 10 Typical failure mode of welded flanges and web cleats connection (BCCF)

3. Classification of the Specimens According to Other Proposals

As already mentioned in the previous paragraph, the EC3 classification system for joints has been recently criticised for several reasons. One of the main drawbacks of the approach is that this considers the stiffness and the strength criteria separately, thus possibly leading to some inconsistencies when both the serviceability and the ultimate state are considered; concerning this point (Nethercot et al., 1998), a unified classification system in which connection stiffness and strength are considered simultaneously, is proposed. Furthermore in Hasan et al. (1998), the weakness of the idea of adopting the stiffness of the beam as the only parameter for defining the initial stiffness of the connection is discussed and the need of defining a non-linear classification system, with no reliance on the beam stiffness is emphasised. However, the definition of a unique approach, fully exhaustive, is not a simple task.

In order to show the differences arising from the application of the different methods, in Figures 8 and 9, the approach proposed by Bjorhovde et al. (1990), quite close to the EC3 one, and the new non-linear system proposed by Hasan et al. (1998) are applied for classifying the TSW and WW large scale connections described in this paper. From Figures 8(b) and 9(b), it derives that the TSW connections can be defined as semi-rigid according to both the two proposal as well as to the EC3. On the contrary for the WW connections (Figure 8(a) and 9(a)), the two systems provide results quite different from the EC3 ones, according which the three connections are all defined as semi-rigid (see Figure 7(b)). Both the systems classify the BCC8 specimen as fully rigid, while the BCC6 and BCC5 specimen behave as semi-rigid joint at serviceability limit state and rigid at the ultimate limit state.
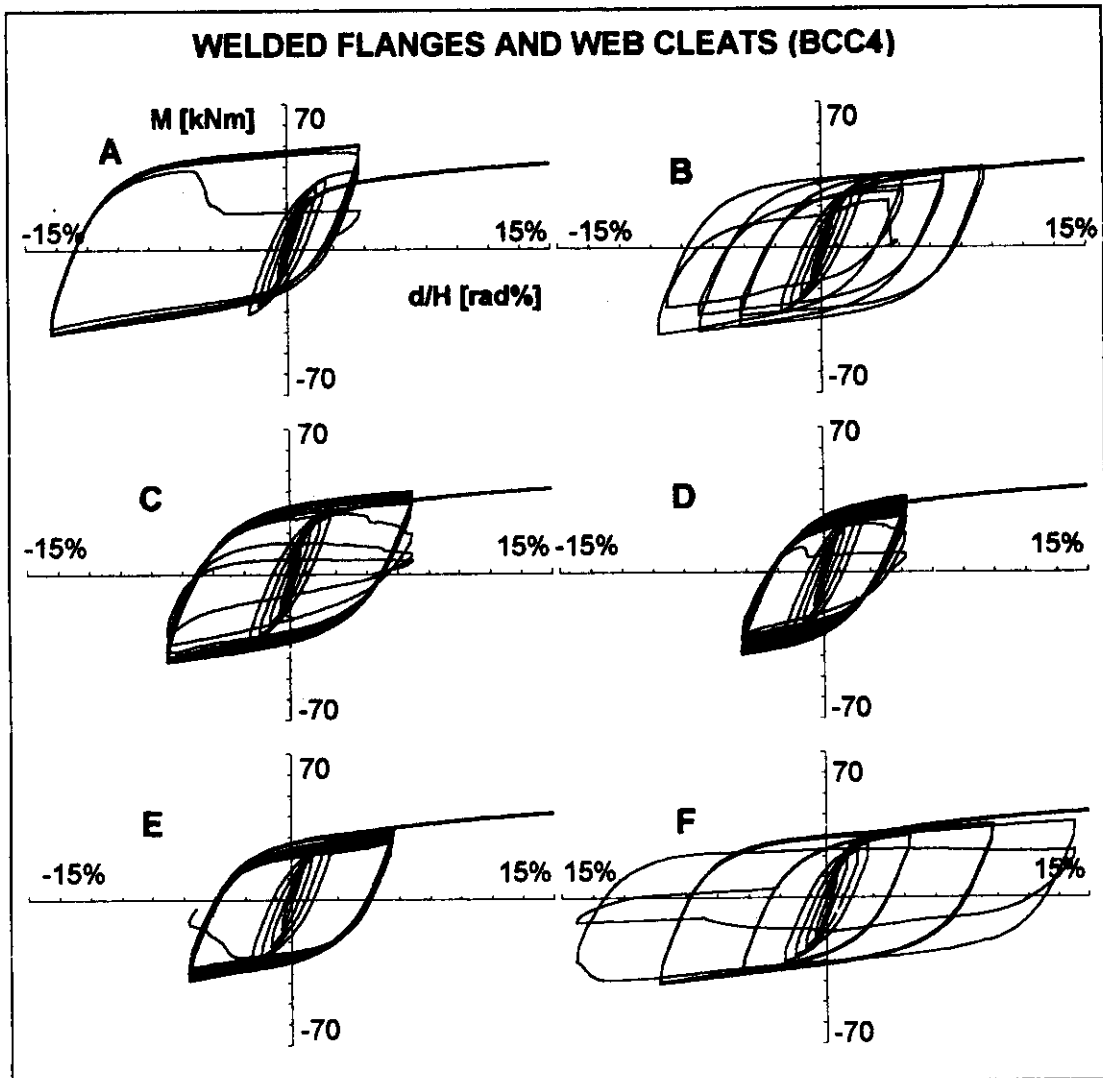

Fig. 12 Hysteresis loops of welded flanges and web cleats connections (BCC4)
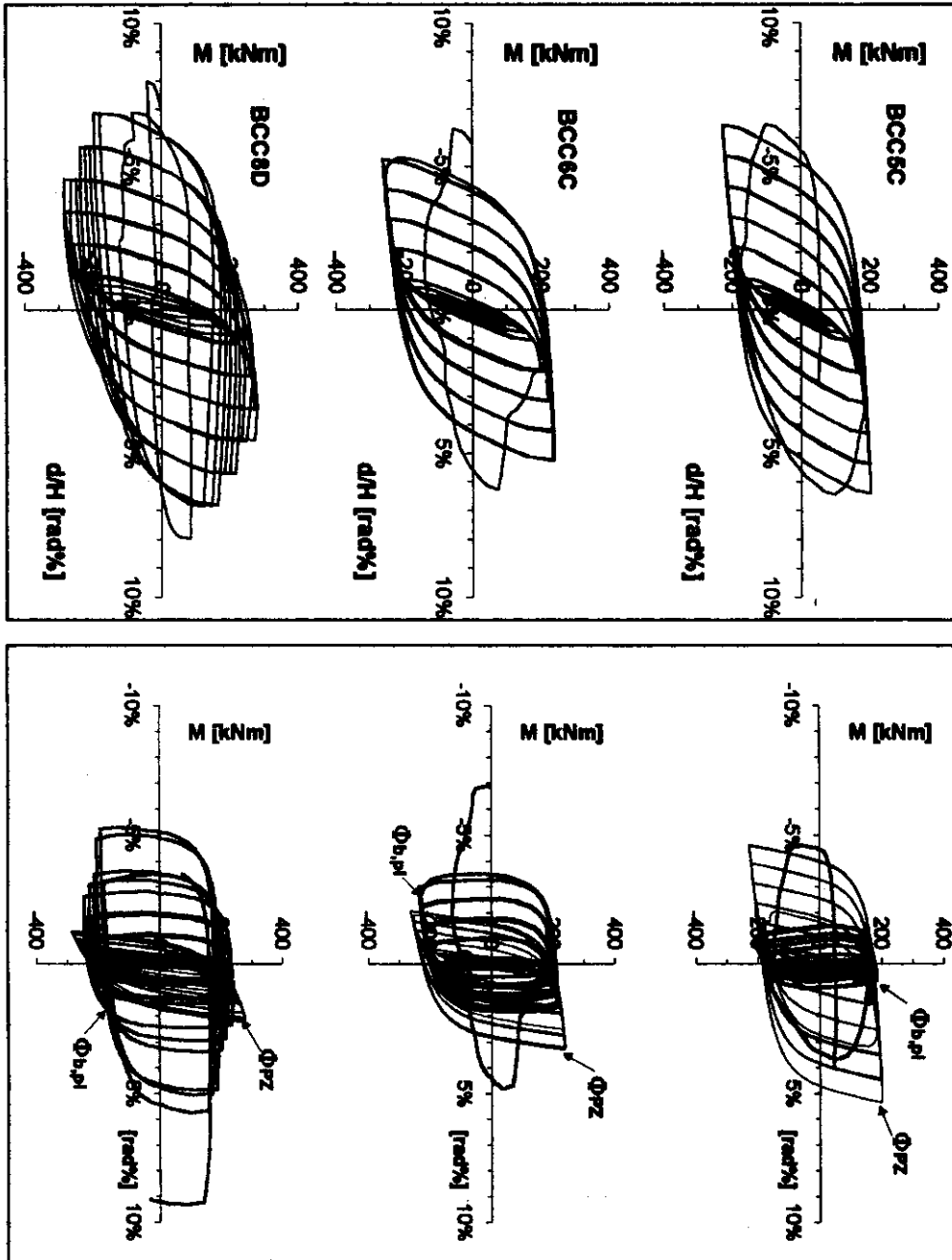
Fig. 13(b) Moment-beam plastic rotation and moment-panel rotation

Fig. 13(a) Moment-global rotation

CYCLIC BEHAVIOUR OF THE WELDED SPECIMENS

1. Small Scale WF Specimens

The cyclic behaviour of the WF BCC4 connection observed throughout the experimental program is characterised by large plastic deformations of the column web panel zone, leading to a significant rotation of the column axis. Final collapse of the connection is achieved due to the formation and growing of cracks, typically starting in the zone adjacent to the welds connecting the beam to the column flanges (Figure 10) and in some cases in the panel zone (Figure 11).

The highly regular and stable hysteresis loops are given in Figure 12. No significant deterioration of mechanical properties has been observed in these connections, as can be derived from the hysteresis loops.

2. Large Scale WW Specimens

In Figure 13(a), the moment-total rotation $(M - d/H)$ experimental curves resulting from the BCC5C, BCC6C and BCC8D tests (cyclic increasing stepwise amplitude) are plotted, while in Figure 13(b), both the corresponding moment (M)–beam plastic rotation $(\Phi_{b,pl})$ and the moment (M)–panel zone rotation (Φ_{PZ}) curves are plotted. The beam plastic rotation has been obtained through the measured displacements at the beam instrumented section by subtracting the contributions of the beam and column elastic rotations as well as of the panel zone distortion.
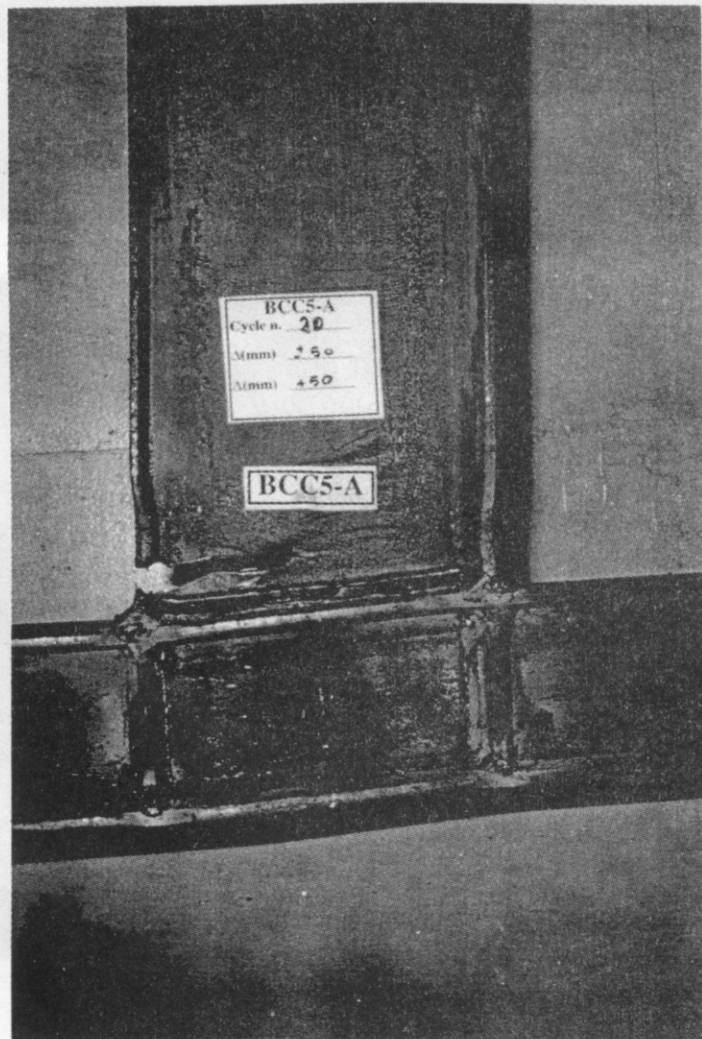

Fig. 14 Failure mode of a fully welded connection (BCC5)
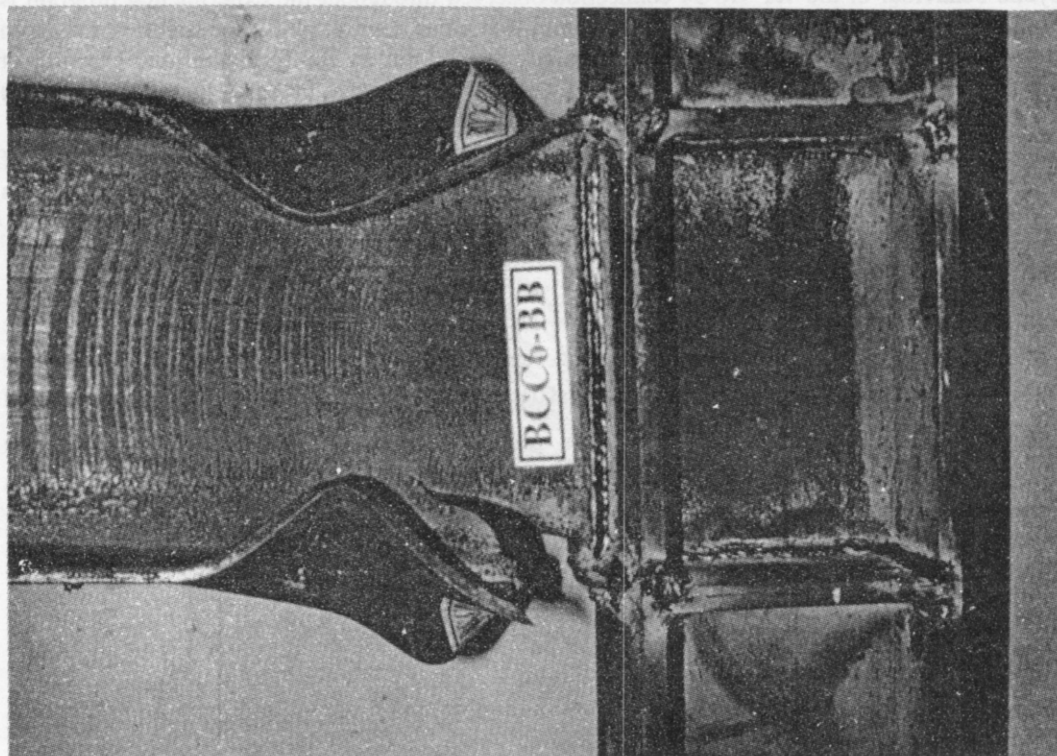
Fig. 15(b) Fracture in the beam flange in the buckled zone (BCC6)
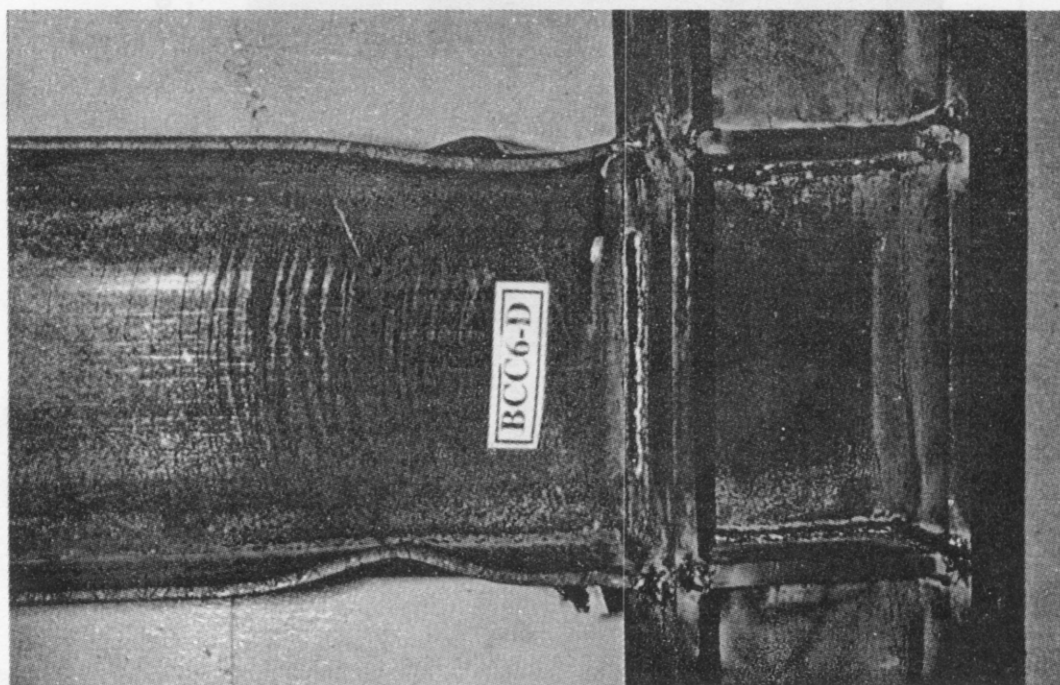
Fig. 15(a) Fracture in the beam flange along the weld line (BCC6)

3. BCC5

As can be derived from the curves reported in Figure 13(a) and (b), and as demonstrated also throughout the experimental program, the cyclic behaviour of the specimen BCC5 is characterised by a great regularity and stability of the hysteresis loops up to failure, with no deterioration of stiffness and strength properties. In the very last cycle, the specimen has collapsed with a sudden and sharp reduction of strength due to fracture initiated in the beam flange and propagated also in the web (Figure 14). During the tests, significant distortion of the joint panel zone has been observed, while not-remarkable plastic deformation occurred in the beam.

4. BCC6

Throughout the test program, two different kinds of cyclic behaviour have been observed for the BCC6 specimens. In some cases the behaviour of the specimens is close to the behaviour observed for the BCC5 type, with almost no deterioration of the mechanical properties up to the last cycle, during which the collapse occurred, due to fracture in the beam flange along the weld line (Figure 15(a)). For the other tests a gradual reduction of the peak moment at increasing number of cycles is evident. In these cases, starting from the very first plastic cycles, local buckling of the beam flanges occurred, and a well-defined plastic hinge has formed in the beam. In these tests, collapse of the specimens was due to fracture of the beam flange in the buckled zone (Figure 15(b)). For all the BCC6 specimens, the contribution of the panel zone deformation has not been as significant as in the BCC5 specimen type.


Fig. 16 Fracture of the beam flange in the buckled zone (BCC8)
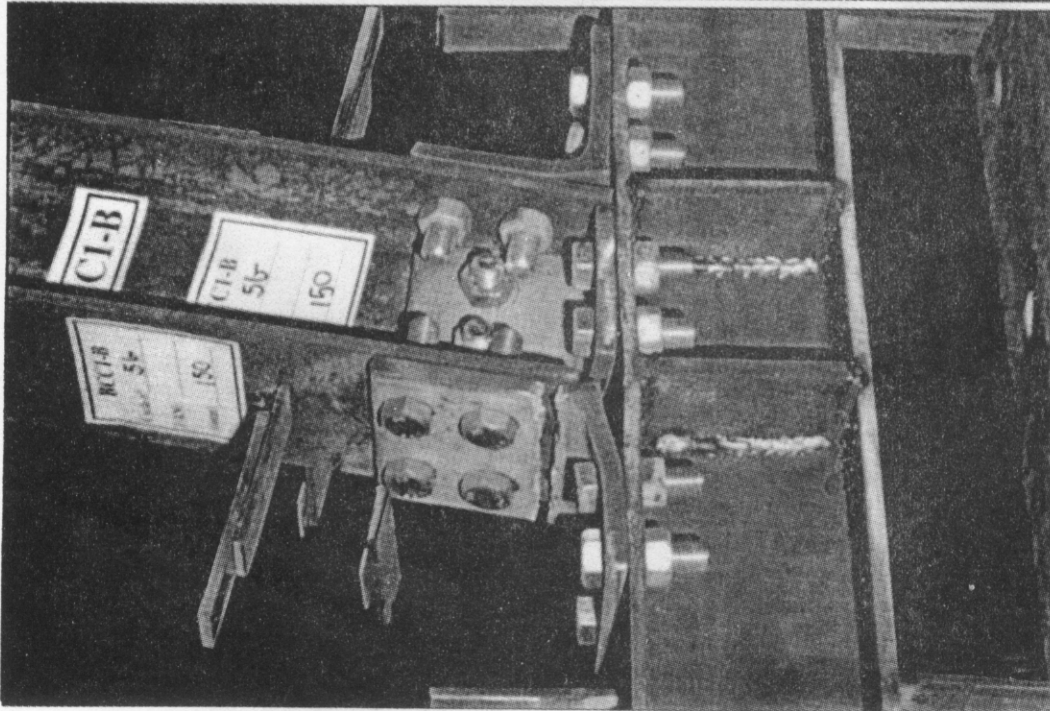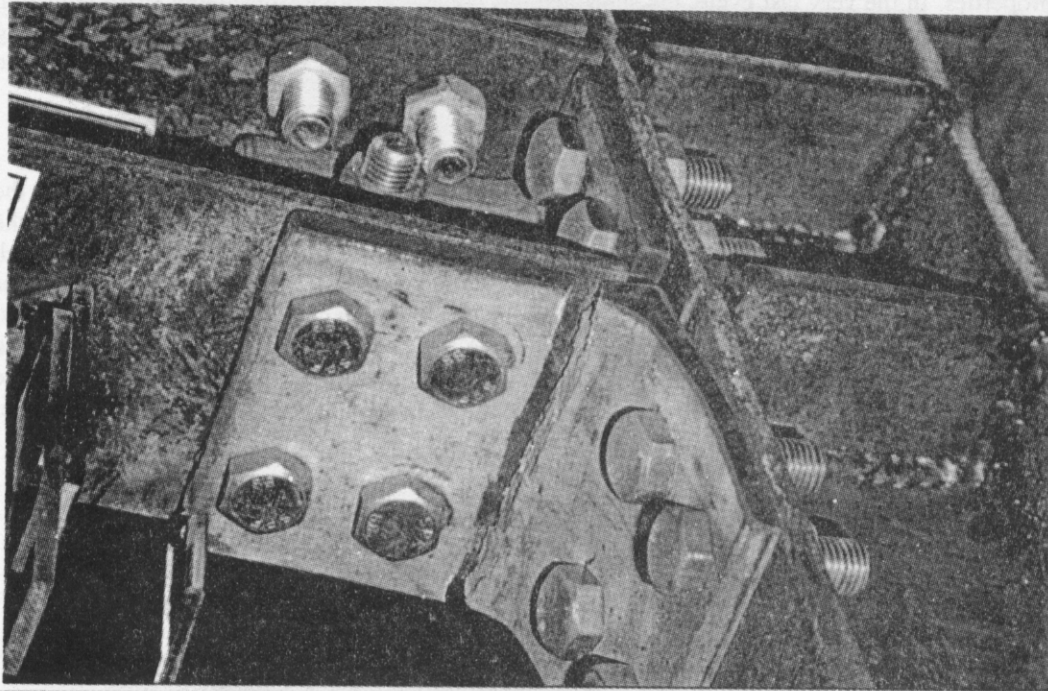
Fig. 17 Failure mode of top and seat with double web angles connections (BCC1)

5. BCC8

The hysteresis loops obtained from the tests on the BCC8 specimens show a gradual reduction of the peak moment starting from the second cycle, where the maximum value of the applied moment has been usually registered. This deterioration of the flexural strength of the connection is related to occurrence and spreading of local buckling in the beam flanges and web. A well-defined plastic hinge in the beam has formed in all the tested specimens, and the collapse of the specimens was due to fracture of the beam flange in the buckled zone (Figure 16) or in the zone close to the weld line. In the specimens BCC8, the panel zone deformation has not been remarkable, and the plastic deformation mainly took place in the beam.

CYCLIC BEHAVIOUR OF THE BOLTED SPECIMENS

1. Small Scale TSW Specimens

The cyclic behaviour of the TSW BCC1 connection observed throughout the experimental program is characterised by significant plastic deformation of the top and bottom angles, mainly occurring in leg adjacent to the column flange. Not-remarkable rotation of the column and distortion of the panel zone have been observed. In all specimens, the failure mode is related to the failure of the weakest component, which is the angle in bending; during all the test, a horizontal crack formed in the top and bottom angles, when cyclically subjected to tension. These cracks, generally located in the leg adjacent to the beam immediately after the fillet, grow as the number of cycles increases and drive the angle to complete fracture (Figure 17).

The moment rotation hysteresis loops obtained from the cyclic tests are provided in Figure 18, where, on each experimental cyclic curve, the experimental monotonic curve is also superimposed. In these curves, the moment M is evaluated at the column centreline, while the rotation is the global interstory drift angle d/H applied to the specimen.

The experimental curves, typical of this type of connection, show pinched hysteresis loops, with a large slip plateau (very low slope of the experimental curve) and subsequent sudden stiffening. This typical behaviour is related to the geometry changes and contact phenomena which arise during the application of the reverse loading; when the specimen position is at $d = 0$, due to the concomitant effects of bolt slippage, hole ovalization and the plastic deformation of the angle legs adjacent to the column flange, the beam is completely separated from the column (gap open). At large applied displacements, which impose large rotations to the connection, the contact between the compression angle and the beam web and the column flange (gap closure) give rise to sudden stiffening of the connection, which is evident in the experimental curves. The different loading histories led to similar results in terms of shape of hysteresis loops. From the curves reported in Figure 18, it is evident that the BCC1 connection is capable of providing large strength and deformation capacities. The significant value of the bending strength exhibited by the specimens (equal to the beam plastic moment $M_{pb} = 40 \, \text{kNm}$ in all but the A, B, and C tests, in which bolts were not preloaded) is related to the geometry of the connection components, as already underlined with reference to the monotonic moment rotation curve.

2. Large Scale TSW Specimens

In Figure 19(a), the moment-total rotation $(M - d/H)$ experimental curves resulting from the BCC9D, BCC7C and BCC10C tests (cyclic increasing stepwise amplitude) are plotted, while in Figure 19(b), both the corresponding moment (M)–beam rotation (Φ_b) and the moment (M)–panel zone rotation (Φ_{PZ}) curves are plotted. As can be derived from the curves reported in Figure 19, the shapes of hysteresis loops of the three TSW specimens are very similar. The cyclic behaviour, the phenomena observed during the tests and the collapse modes are the same for the three specimen series; thus, the following unique paragraph is devoted to describe the above issues for the three specimens.
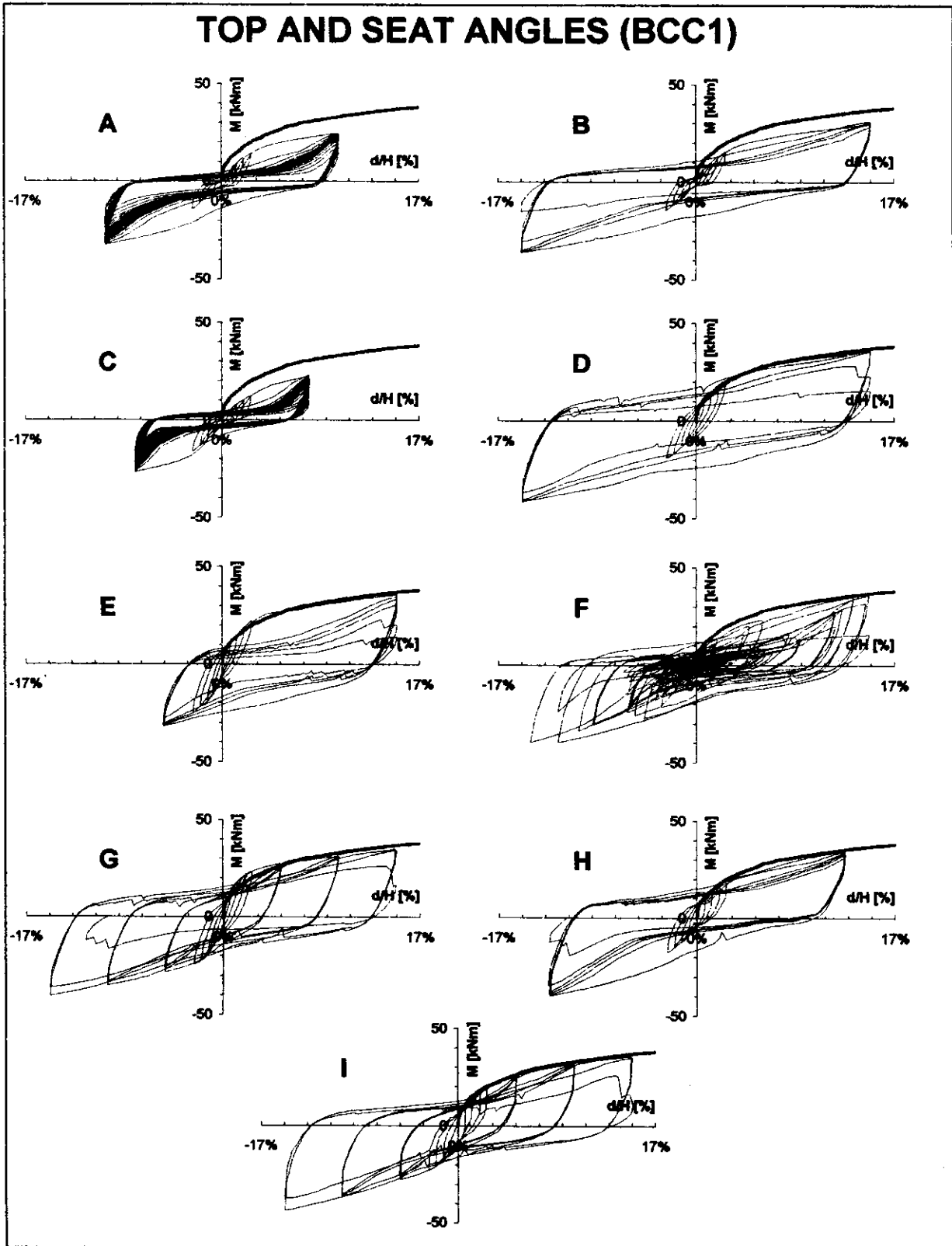
Fig 18 Hysteresis loops of top and seat with double web angles connections (BCC1)
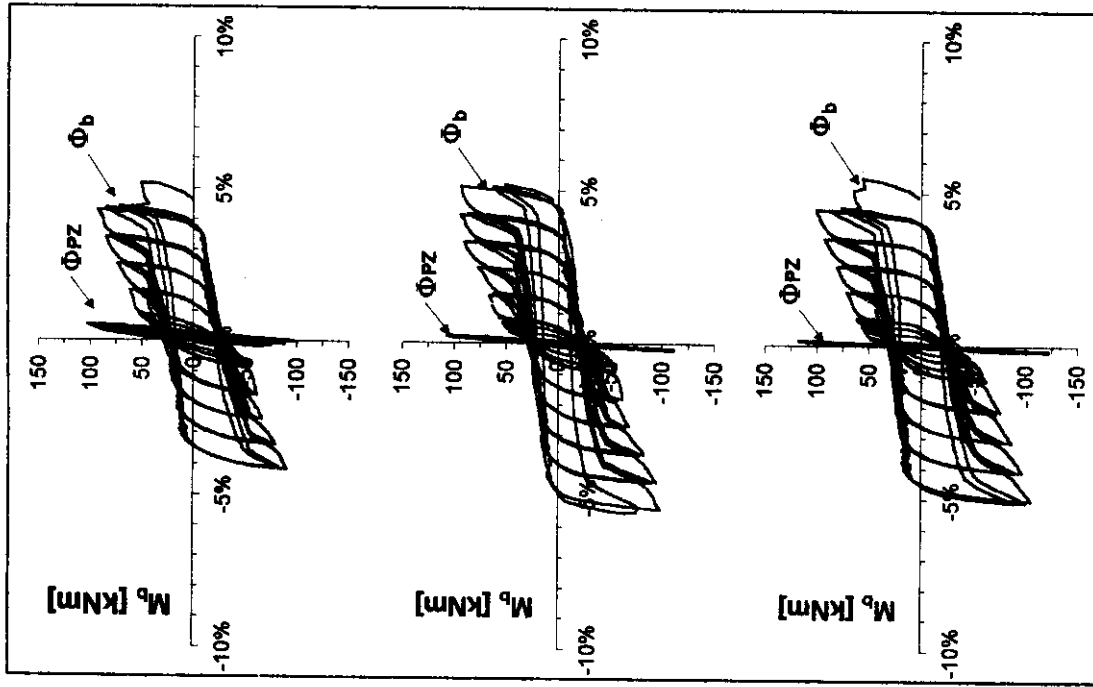
Fig. 19(b) Moment-beam plastic rotation and moment-panel rotation
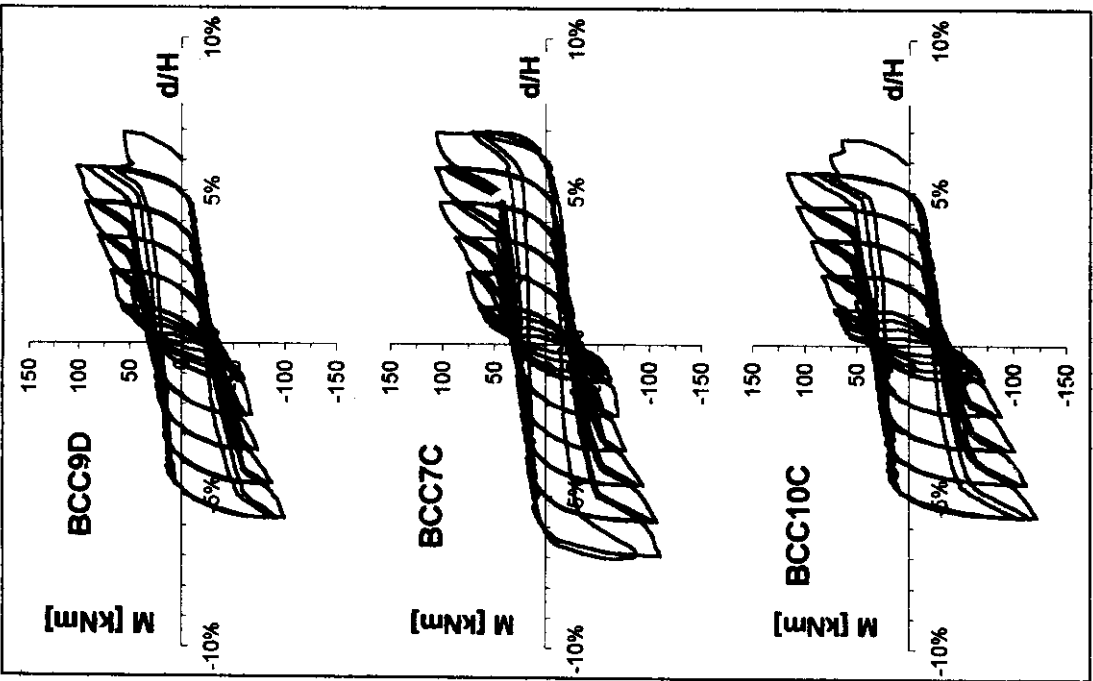
Fig 19(a) Moment-global rotation

3. BCC9 / BCC7 / BCC10

The cyclic behaviour of the TSW connections is characterised by bolt slippage and yielding and spreading of plastic deformation in the top and bottom angles, cyclically subjected to tension. Plastic ovalization of the bolt holes has also been observed mainly in the leg of the angle adjacent to column flange. The experimental curves show the same typical, pinched hysteresis loops, as observed for the small scale BCC1 specimens, with a large slip plateau and subsequent sudden stiffening, due to the contact between the angles and the column flange. No significant rotation of the column and distortion of the panel zone have been observed throughout the experimental tests carried out on the three specimens. At each step on the test, slight deterioration of the joint resistance in the three applied cycles can be observed in the experimental curves, mainly due to yielding and spreading of plastic deformation in the top and bottom angles, cyclically subjected to tension. In the entire test carried out on the three specimen series, the collapse of the connection occurred due to fracture in the leg angle located on the beam flange, immediately after the fillet (Figure 20). Negligible scatters can be observed in the moment capacity of the three connection series, as it is expected, since the inelastic behaviour of the connection is governed by the angle. Also, the maximum values of global rotation experienced by the specimens is the same for the BCC9 and BCC10 series, and slightly larger for the BCC7 one.
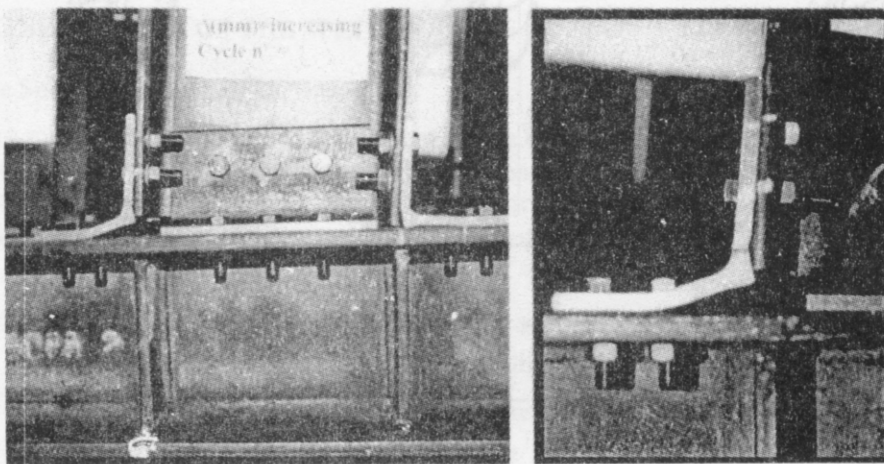

Fig. 20 Typical failure mode of top and seat with web angle connections (BCC10)

SUMMARY AND CONCLUDING REMARKS

In this paper an overview of different experimental programs, carried out in the last years at IST of Lisbon, on different types of beam-to-column connections, has been provided. In particular, the tests on top and seat with web angles connections and on welded connections have been analysed. The great deal of experimental results obtained in these researches have been presented in terms of hysteresis loops and collapse modes and, due to space limitation, only some major aspects have been evidenced in this paper.

In particular, a significant scale effect, resulting from the comparison between small size and large size specimens, has been found to affect the experimental behaviour of both bolted and welded connections.

The major design aspects governing the cyclic and the monotonic behaviour of bolted and welded connections have been evidenced against experimental results, as reported in the following.

1. Bolted Connections

It has been shown that, as a consequence of design choices, the panel zone does not affect the behaviour of the bolted (TSW) connections, which instead is mainly related to the geometry and strength properties of the flange angles. The test results also confirm major findings reported in the bibliography on the cyclic behaviour of bolted angles connections (Azizinamini and Radziminski, 1989; Mander et al.; 1994; Calado and Ferreira, 1994; Kukreti and Abolmaali, 1999), where it is stated that connections for

which the flange angle is the weakest component and the design is aimed at excluding bolt slippage at service load level, can be very stable and highly dissipative and can provide a non-negligible moment capacity.

2. Welded Connections

In the case of welded connections, the relative strength ratios of beam, column and panel zone has demonstrated to affect at a large extent all the response parameters (stiffness, strength and deformation capacity). A significant contribution of panel zone deformation has been observed throughout the tests, suggesting the possibility of utilising the joint panel for providing energy dissipation and stable behaviour of the connections even at large number of cycles. Weak panel zone, however, gives rise to inelastic deformation mode of the beam-column subassemblage which produces high stress concentrations at the beam (flanges and web) to column welded zones, which finally drive the specimen to brittle collapse mode. These results confirm some major findings reported in El-Tawil et al. (1999) and Lu et al. (2000). In El-Tawil et al. (1999), on the basis of FEM analyses results, it is emphasised that although weak-panel design of the beam-to-column welded connections can substantially reduce beam plastic rotation demands and effectively contribute to global connection ductility, the stress state arising at high levels of applied rotation increases the potentials for brittle fracture collapse mode of the connection. In Lu et al. (2000), based both on experimental tests and FEM theoretical studies, it is found that weak column panel specimens (with PZ contributing at 70% to the total plastic rotation of the specimen) show brittle failure modes, with no previous deterioration of the strength capacity, due to fracture in the beam web weld and beam bottom flange.

ACKNOWLEDGMENTS

REFERENCES

1. Astaneh-Asl, A. (1995). "Seismic Design of Bolted Steel Moment-Resisting Frames", Steel Tips, Structural Steel Educational Council, Moraga, California, U.S.A.

2. Azizinamini, A. and Radziminski, J.B. (1989). "Static and Cyclic Performance of Semi-Rigid Steel Beam-to-Column Connections", Journal of Structural Engineering, ASCE, Vol. 115, No. 12.

3. Bjorhovde, R., Colson, A. and Brozzetti, J. (1990). "Classification System for Beam-to-Column Connections", Journal of Structural Engineering, ASCE, Vol. 116.

4. Calado, L. and Ferreira, J. (1994). "A Numerical Model for Predicting the Cyclic Behaviour of Steel Beam-to-Column Joints", Proc. of the 10th European Conference on Earthquake Engineering, Vienna, Austria.

5. Calado, L., Mele, E. and De Luca, A. (1999a). "Cyclic Behaviour of Steel Semi-Rigid Beam-to-Column Connections", Journal of Structural Engineering, ASCE, Submitted for Publication.

6. Calado, L., Mele, E. and De Luca, A. (1999b). "Experimental Investigation on the Cyclic Behaviour of Welded Beam-to-Column Connections", Proc. of the 2nd European Conference on Steel Structures, Eurosteel 1999, PRAHA, Czech Republic, Paper No. 215.

7. Calado, L. and Mele, E. (2000). "Experimental Behaviour of Steel Beam-to-Column Joints: Fully Welded vs Bolted Connections", Proc. of the 12th World Conference on Earthquake Engineering, Auckland, New Zealand, Paper No. 2570/6/A.

8. CEN (1997). "Annexure J: Joints in Building Frames", TC250/SC3-PT9, Approved Draft of Eurocode 3, Part 1.1.

9. El-Tawil, S., Vidarsson, E., Mikesell, T. and Kunnath, S.K. (1999). "Inelastic Behaviour and Design of Steel Panel Zones", Journal of Structural Engineering, ASCE, Vol.125, No. 2.

10. Elnashai, A.S., Elghazouli, A.Y. and Denesh-Ashtiani, F.A. (1998). "Response of Semi-Rigid Steel Frames to Cyclic and Earthquake Loads", Journal of Structural Engineering, ASCE, Vol.124, No. 8.

11. Hasan, R., Kishi, N. and Chen, W.F. (1998). "A New Non-Linear Connection Classification System", Journal of Constructional Steel Research, Vol. 47.

12. Kishi, N. and Chen, W.F. (1990). "Moment Rotation Relations of Semi-Rigid Connections with Angles", Journal of Structural Engineering, ASCE, Vol. 116.

13. Kukreti, A.R. and Abolmaali, A.S. (1999). "Moment-Rotation Hysteresis Behaviour of Top and Seat Angle Steel Frame Connections", Journal of Structural Engineering, ASCE, Vol.125, No. 8.

14. Lu, L.W., Ricles, J.M., Mao, C. and Fisher, J.W. (2000). "Critical Issues in Achieving Ductile Behaviour of Welded Moment Connections", Journal of Constructional Steel Research, Vol. 55.

15. Mander, J.B., Chen, S.S. and Peckan, G. (1994). "Low-Cycle Fatigue Behaviour of Semi-Rigid Top-and-Seat Angle Connections", Engineering Journal, AISC, No. 3.

16. Mele, E., Calado, L. and Pucinotti, R. (1997). "Indagine Sperimentale Sul Comportamento Ciclico di Alcuni Collegamenti in Acciaio", Proc. of the 8th ANIDIS – Italian National Association of Earthquake Engineering, Taormina, Italy (in Italian).

17. Nethercot, D.A., Li, T.Q. and Ahmed, B. (1998). "Unified Classification System for Beam-to-Column Connections", Journal of Constructional Steel Research, Vol. 45.

18. Roeder, C.W. (1998). "Design Models for Moment Resisting Steel Constructions", Proc. of the SEWC – Structural Engineering World Wide Conference, San Francisco, Paper T158-4.